ACS APPLIED MATERIALS & INTERFACES

Research Article

Cite This: ACS Appl. Mater. Interfaces 2018, 10, 32047−32057

www.acsami.org

Temperature-Induced Denaturation of BSA Protein Molecules for Improved Surface Passivation Coatings

Jae Hyeon Park,[†] Joshua A. Jackman,[†] Abdul Rahim Ferhan,[†] Gamaliel Junren Ma,[†] Bo Kyeong Yoon,[†] and Nam-Joon Cho*[,†,‡]

[†]School of Materials Science and Engineering, Nanyang Technological University, 50 Nanyang Drive, 637553 Singapore

[‡]School of Chemical and Biomedical Engineering, Nanyang Technological University, 62 Nanyang Drive, 637459 Singapore

Supporting Information

ABSTRACT: Bovine serum albumin (BSA) is the most widely used protein for surface passivation applications, although it has relatively weak, nonsticky interactions with hydrophilic surfaces such as silica-based materials. Herein, we report a simple and versatile method to increase the stickiness of BSA protein molecules adsorbing onto silica surfaces, resulting in up to a 10-fold improvement in blocking efficiency against serum biofouling. Circular dichroism spectroscopy, dynamic light scattering, and nanoparticle tracking analysis showed that temperature-induced denaturation of BSA proteins in bulk solution resulted in irreversible unfolding and protein oligomerization, thereby converting weakly adhesive protein monomers into a more adhesive oligomeric form. The heat-treated, denatured BSA oligomers remained stable after cooling. Room-temperature quartz crystal microbalance-dissipation and localized surface plasmon resonance experiments revealed that denatured BSA oligomers adsorbed more quickly and in larger mass quantities onto silica surfaces than native BSA monomers. We also determined that the larger surface contact area of denatured BSA oligomers is an important factor contributing to their more adhesive character. Importantly, denatured BSA oligomers were a superior passivating agent to inhibit biofouling on silica surfaces and also improved Western blot application performance. Taken together, the findings demonstrate how temperature-induced denaturation of BSA protein molecules can lead to improved protein-based coatings for surface passivation applications.

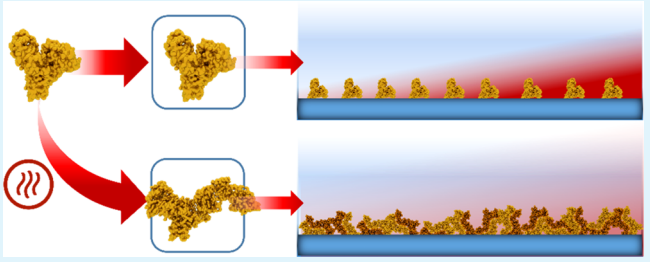

KEYWORDS: *surface passivation, biofouling, bovine serum albumin, protein adsorption, quartz crystal microbalance-dissipation, localized surface plasmon resonance*

INTRODUCTION

The design of biologically inert surfaces and interfaces is a key objective of materials science and holds broad relevance for numerous applications. For example, preventing the nonspecific adsorption of fouling molecules onto measurement platforms is critical for sensor performance, while limiting protein adsorption onto and immune recognition of medical implant surfaces can improve biocompatibility.[1−3] In the chemical and materials science fields, a wide range of synthetic and bioinspired polymeric coatings, including hydrophilic polymer brushes, have been employed to fabricate nonfouling interfaces and are the subject of intense research and development.[4−9] However, in part due to their simplicity and versatility as well as historical precedent, protein-based coatings remain the "gold standard" for many biological applications, such as enzyme-linked immunosorbent assay, and bovine serum albumin (BSA) is the most common passivating agent for such applications to prevent nonspecific binding of various fouling molecules.[10−14] Curiously, there are many different types of processed BSA available and scant discussion in the scientific literature about which type of BSA is most suitable for surface passivation applications or how existing BSA samples can be processed to improve blocking performance. From a materials science perspective, this knowledge gap is particularly striking because BSA has relatively weak, nonsticky interactions with commonly used surfaces, such as silica-based materials,[15] and there is significant opportunity to improve blocking performance based on exploiting fundamental steps in the protein adsorption process to promote stronger protein−surface interactions. An ideal passivation layer should be dense to maximize surface coverage and minimize biofouling,[16] while the passivating molecules should adhere irreversibly to surfaces to quickly achieve saturation coverage in coating protocols.[17]

To this end, noncovalent protein adsorption is one of the simplest and most versatile options to fabricate protein-based coatings. Protein adsorption typically begins with the adhesion of contacting protein molecules to a material surface. The

Received: August 10, 2018
Accepted: September 4, 2018
Published: September 4, 2018

DOI: 10.1021/acsami.8b13749
ACS Appl. Mater. Interfaces 2018, 10, 32047−32057

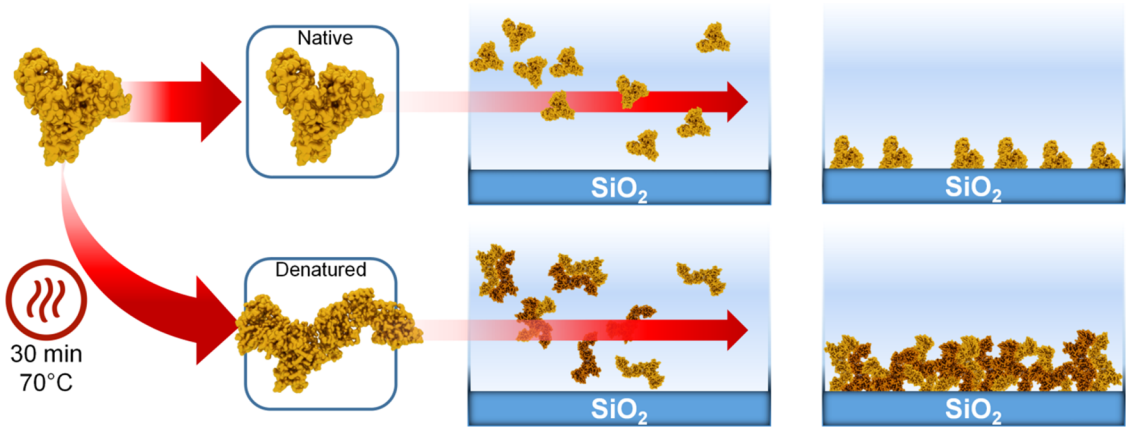

Figure 1. Schematic illustration of denatured BSA protein-based surface passivation strategy. When BSA is thermally denatured, it undergoes irreversible conformational changes that persist after cooling back to room temperature. The denatured BSA molecules have altered conformational properties in bulk solution that promote greater irreversible adsorption onto silica surfaces. Compared to native BSA, it is proposed that denatured BSA can form denser coatings that are superior for surface passivation applications.

initial adsorption step is strongly influenced by the surface area of the contact region between a protein molecule and the material surface.[18−20] This step is followed by surface-induced denaturation of adsorbed protein molecules, which is governed by protein−protein and protein−surface interactions.[21,22] Surface-induced denaturation itself is a thermodynamically favorable process that involves protein unfolding and resulting conformational changes, which can increase the number of contact sites between individual protein molecules and the material surface.[3] The number and adhesion strength of contact sites between a protein molecule and a material surface can affect whether or not a bound protein molecule will remain adsorbed. Experimentally, Karlsson et al. demonstrated how engineered mutants of human carbonic anhydrase II with more extensive denaturation in the adsorbed state exhibited greater adsorption irreversibility on all tested surface types (negatively charged, positively charged, hydrophilic, and hydrophobic).[23] Goli et al. also demonstrated how chemically or thermally denatured proteins such as lysozyme and fibrinogen adsorb strongly onto hydrophobic surfaces.[24,25] Such insights indicate that modulating the conformational properties of a protein in bulk solution can promote greater irreversible adsorption onto solid surfaces, providing a possible design cue to improve BSA protein adhesion for surface passivation applications.

To date, a few BSA adsorption studies have fundamentally investigated how solution-phase denaturation affects protein adsorption. Damodaran and Song reported that chemical denaturation of BSA molecules by urea treatment yielded partially denatured BSA, and the extent of denaturation (interpreted by the percentage decrease in helicity) correlated with the adsorption rate at the air−liquid interface compared to native BSA.[26] To explain this observation, the authors suggested that denatured BSA might have a lower desorption rate than native BSA, possibly indicating a stronger protein−surface interaction. In another example, Shirahama and Suzawa showed that there was greater uptake of heat-denatured BSA to polymer lattices.[27] Building on these works, we have recently observed that temperature-induced reversible conformational changes in monomeric BSA molecules (decreased helicity) are correlated with the extent of surface-induced denaturation, providing direct experimental evidence of a relationship between the helicity of individual protein molecules in bulk solution and greater surface-induced denaturation in the adsorbed state.[28] Collectively, the existing fundamental works support that the conformational properties of BSA proteins in bulk solution influence protein adsorption and surface-induced denaturation, highlighting the potential benefits of intentionally modulating the structural and conformational properties of BSA molecules to promote greater irreversible adsorption and improved surface passivation.

Herein, by utilizing thermal denaturation to purposefully modulate the structural and conformational properties of BSA molecules in bulk solution, we report a simple and versatile method to increase the stickiness of BSA adsorption onto silica surfaces, resulting in up to a 10-fold improvement in blocking efficiency against serum biofouling and other application possibilities (Figure 1). Our findings validate how the conformation of BSA protein molecules in bulk solution is intimately linked with functional properties in the adsorbed state, as verified by multiple experimental approaches, including solution-phase structural and size characterization, surface-sensitive techniques for adsorption profiling, and direct evaluation of blocking efficiency against surface biofouling by whole fetal bovine serum (FBS). In addition to improved surface passivation, the use of denatured BSA streamlined the coating procedure by shortening the required incubation time. While the interaction of denatured BSA with material interfaces has been shown to improve luminescent properties[29,30] and charge-transfer properties[31−33] as well as stabilize nanomaterials,[34,35] our work is the first report demonstrating how denatured BSA is superior to inhibit fouling by serum components, in terms of both blocking efficiency and coating time.

MATERIALS AND METHODS

Reagents. Bovine serum albumin (A2153), sodium dodecyl sulfate (SDS, L4390), and sodium chloride (NaCl, BioXtra) were purchased from Sigma-Aldrich (St. Louis, MO). Tris(hydroxymethyl)aminomethane (Tris) was purchased from Amresco (Solon, OH). Ethanol (absolute grade, EMSURE) and hydrochloric acid (HCl, EMSURE) were purchased from Merck Millipore (Billerica, MA). Silica nanoparticles were purchased from nanoComposix (San Diego, CA), and normal human serum and complement iC3b monoclonal antibody were obtained from Complement Technology (Tyler, TX) and Thermo Fisher Scientific (Waltham, MA), respectively. All other Western blotting reagents

DOI: 10.1021/acsami.8b13749
ACS Appl. Mater. Interfaces 2018, 10, 32047−32057

were obtained from Bio-Rad (Hercules, CA). All chemicals were used as received without further purification.

Sample Preparation. A buffer solution consisting of 10 mM Tris (pH 7.5) with 150 mM NaCl was prepared using deionized water filtered through a Milli-Q water purification system (18.2 MΩ cm resistivity at 24 °C), followed by titration with 1 M HCl. A stock solution of BSA protein was prepared by dissolving the lyophilized protein in Tris−HCl buffer solution at a nominal protein concentration of 100 μM. The protein concentration was verified by UV−vis spectroscopy (S-220, Boeco, Germany) at 280 nm wavelength. Where applicable, thermal denaturation was performed by heating 100 μM BSA in a water bath at 70 °C for 30 min. Lower bulk concentrations of protein were prepared by diluting the 100 μM protein solution with Tris−HCl buffer solution as appropriate.

Circular Dichroism (CD) Spectroscopy. The secondary structures of native and thermally denatured BSA were investigated by employing CD spectroscopy. CD spectra of the protein solutions (25 μM concentration) were measured with an AVIV model 420 spectrometer (AVIV Biomedical, Lakewood, NJ) using a quartz cuvette of 1 mm path length. The spectra were recorded in triplicate from 190 to 260 nm in 0.5 nm intervals with a 4 s averaging time and 1.0 nm bandwidth. More details on data analysis are provided in the Supporting Information.

Dynamic Light Scattering (DLS). A NanoBrook 90Plus particle size analyzer (Brookhaven Instruments, Holtsville, NY) was employed to measure the average hydrodynamic diameter and polydispersity of BSA protein molecules in solution. All measurements were performed with a 658.0 nm monochromatic laser and recorded at a scattering angle of 90°. Analysis of the intensity autocorrelation function was done by the BIC Particle Sizing software package to obtain the intensity-weighted Gaussian size distribution, and the average hydrodynamic diameter is reported from $n = 5$ technical replicates. All measurements were performed at 25 °C in a temperature-controlled measurement chamber.

Nanoparticle Tracking Analysis (NTA). Nanoparticle tracking analysis (NTA) of BSA protein molecules diffusing under Brownian motion in bulk solution was performed using a NanoSight LM10 instrument (Malvern Instruments, Malvern, U.K.), as previously described.[36] Briefly, protein samples were first diluted and manually introduced into the sample chamber by using a sterile disposable syringe. A 405 nm laser was then used to illuminate the sample. The light undergoes Rayleigh scattering by the diffusing protein molecules in bulk solution, and the scattered light was observed by an optical microscope (20× magnification) and recorded by a built-in sCMOS camera at a rate of 25 frames s^{-1} for a 3 min duration. The recorded data were then analyzed using the NTA 3.1 Build 3.1.46 software package. The Brownian motion of individual protein molecules in bulk solution was tracked in real time, and the Stokes−Einstein equation was used to calculate the hydrodynamic diameter of protein molecules. All measurements were conducted at room temperature.

Quartz Crystal Microbalance-Dissipation (QCM-D) Measurements. Protein adsorption onto silica surfaces was investigated by employing a Q-Sense E4 instrument (Biolin Scientific AB, Stockholm, Sweden), as previously described.[37] AT-cut quartz crystals with a 5 MHz fundamental frequency were used for all experiments, and were coated with a 50 nm thick layer of silica (QSX 303, Biolin Scientific AB). Immediately before experiment, each sensor chip was sequentially rinsed with Milli-Q water and ethanol and dried under a gentle stream of nitrogen gas. The sensor chips were then treated with oxygen plasma (PDC-002, Harrick Plasma, Ithaca, NY) at maximum radiofrequency power for 2 min. The treated sensor chips were enclosed within the measurement chambers, and liquid samples were introduced via a peristaltic pump (ISM833C, Ismatec SA, Switzerland) at a flow rate of 100 μL min^{-1}. Changes in resonance frequency (Δf) and energy dissipation (ΔD) of the sensor chips were recorded at multiple odd overtones, and all measurements were conducted at 25 °C. The normalized data at the fifth overtone (25 MHz) are reported. The QCM-D measurement data were analyzed by the Voigt−Voinova model[38] to extract the effective film thickness. For modeling analysis, the adsorbed protein layer was assumed to form a single, homogenous layer with a uniform effective density of 1300 kg m^{-3}, and the density and viscosity of the bulk aqueous solution were fixed at 1000 kg m^{-3} and 0.001 Pa s^{-1}, respectively.

Localized Surface Plasmon Resonance (LSPR) Measurements. An Insplorion XNano instrument (Insplorion AB, Gothenburg, Sweden) was employed to perform ensemble-averaged LSPR measurements in optical transmission mode, as previously described.[39] The sensor chips (Insplorion AB) consisted of well-separated (~8% surface coverage) gold nanodisk arrays on a fused silica substrate, as fabricated by hole-mask colloidal lithography.[40] The sensor surface was coated with a thin, conformal layer of silicon nitride (~10 nm thick). Immediately before experiment, the sensor chip was sequentially rinsed with Milli-Q water and ethanol and dried under a gentle stream of nitrogen gas, followed by treatment with oxygen plasma at maximum radiofrequency power for 2 min (PDC-002, Harrick Plasma). The latter process results in the formation of a silica layer on the sensor surface. After surface treatment, the sensor chips were enclosed within a microfluidic flow-through chamber and liquid samples were introduced via a peristaltic pump at a flow rate of 50 μL min^{-1}. Extinction spectra were recorded and analyzed in real time (1 Hz resolution) by using the Insplorer software (Insplorion AB), and the centroid position[41] in the extinction spectrum was determined by high-order polynomial fitting.

SDS-Polyacrylamide Gel Electrophoresis (PAGE) and Western Blot Analysis. Silica nanoparticles were incubated in 1% normal human serum for 30 min at 37 °C. After incubation, the samples were centrifuged at 16 000*g* for 5 min and the supernatants were collected in separate tubes mixed with 4× Laemmli sample buffer. The samples were then boiled for 5 min at 95 °C and loaded into the wells of 8% polyacrylamide gels along with appropriate controls. SDS-PAGE was performed at 100 V for 2 h and then the protein bands were transblotted onto nitrocellulose membranes at 300 mA for an additional 2 h. The transblotted membranes were blocked by TBST (Tris-buffered saline with 0.1% Tween 20) buffer solution that contained either 3% native BSA monomers or 3% predenatured BSA oligomers. Before experiment, the predenatured BSA oligomers were prepared by incubation at 70 °C for 1 h before cooling to room temperature. After the blocking step, the transblotted membranes were incubated with primary iC3b antibodies (diluted at 1:500 in blocking buffer) for 1 h. After three subsequent washes with TBST, the membranes were incubated with horseradish peroxidase-conjugated secondary antibodies (diluted at 1:2000 in blocking buffer) for 1 h. The membranes were washed four times with TBST, and the protein bands were detected using an enhanced chemiluminescent kit (Bio-Rad) and imaged with an Amersham Imager 600 (GE Healthcare, Chicago, IL).

RESULTS AND DISCUSSION

Heat Denaturation of BSA Protein. Heat denaturation of BSA protein molecules in bulk solution is a well-studied phenomenon and was utilized here to prepare denatured BSA with altered conformational properties. With increasing temperature, BSA molecules undergo a series of reversible and/or irreversible conformational changes, whereby individual molecules transition from α-helical to β-sheet motifs before partially unfolding to yield random coil structures that can oligomerize.[42−46] We first characterized how heat treatment processing affects the secondary structure and size of protein molecules in bulk solution. Circular dichroism (CD) spectroscopic measurements showed that BSA molecules at 25 °C had 66% fractional helicity, while the helicity of BSA molecules at 70 °C decreased to 53% (Figure 2). The decrease in helicity is consistent with BSA molecules undergoing partial unfolding, and the corresponding magnitude is comparable to the results obtained in previous reports.[43−45] The heated protein solution was then cooled to room temperature, and subsequent measurements at 25 °C indicated that the

DOI: 10.1021/acsami.8b13749
ACS Appl. Mater. Interfaces 2018, 10, 32047−32057

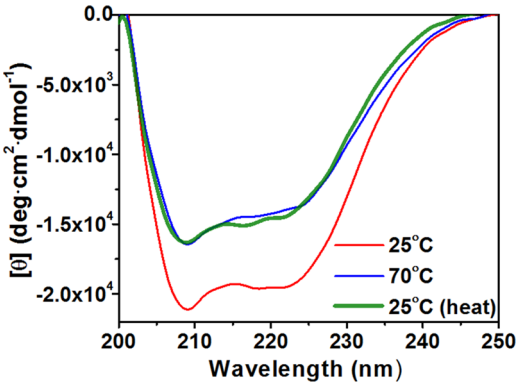

Figure 2. Effect of heat treatment on BSA protein secondary structure in bulk solution. Circular dichroism spectra of BSA protein in native state at 25 °C (red), denatured state at 70 °C (blue), and denatured state at 25 °C after heating and cooling (green). The data are expressed as mean residue ellipticity units (θ).

fractional helicity remained at 53%. This finding verified that thermal denaturation induces irreversible conformational changes in the BSA protein structure and confirmed the presence of denatured BSA in bulk solution at room temperature.

The change in secondary structure of denatured BSA molecules in bulk solution was accompanied by a change in the size distribution of the protein molecules, as corroborated by dynamic light scattering (DLS) and nanoparticle tracking analysis (NTA) measurements to investigate the corresponding changes in protein size distribution (Figure 3). Room-temperature DLS measurements indicated that the hydrodynamic diameter of native and heat-pretreated BSA protein molecules in solution were 8.2 ± 0.1 and 43.8 ± 4.7 nm, respectively (Figure 3a). The measured sizes are consistent with native BSA protein molecules existing in the monomeric state, while denatured BSA proteins assume an oligomeric state. This finding agrees well with literature reports, indicating that heat-induced irreversible conformational changes in BSA molecules are accompanied by oligomerization as a means to stabilize newly exposed hydrophobic regions.[22,46−49] To confirm the presence of BSA oligomers, the size distribution of heat-pretreated, denatured BSA was measured by NTA and it was determined that denatured BSA oligomers have diameters of around 50−150 nm (Figure 3b).[36] The denatured BSA oligomers remained stable in size over time, supporting that the oligomeric state minimizes the exposure of hydrophobic regions. Taken together, the DLS and NTA findings are consistent with the CD spectroscopic measurements and indicated that heat pretreatment of BSA protein molecules at 70 °C resulted in the irreversible formation of denatured BSA oligomers with altered size and conformational properties.

QCM-D Measurements on Native and Denatured BSA Adsorption. QCM-D experiments were next conducted to compare the room-temperature adsorption kinetics of native and denatured BSA on silica surfaces (Figure 4). Silica is a hydrophilic material, and protein adsorption onto silica surfaces is driven by a combination of long-range electrostatic forces and shorter-range hydrogen bonding and van der Waals interactions.[3,50,51]

QCM-D resonance frequency (Δf) and energy dissipation (ΔD) shifts were tracked as a function of time to characterize the mass and the viscoelastic properties of the adsorbed protein layer, respectively. A measurement baseline was first established in aqueous buffer solution, and then 100 μM of native or denatured BSA was injected at t = 8 min. The tested protein concentration is within the typical range of blocking protocols,[17,52] while the ionic strength condition (150 mM NaCl) is also representative of conventional blocking buffers. For both proteins, a monotonic decrease in the Δf signal was observed. At saturation, a Δf shift of around −37 Hz was observed for native BSA monomers, while a larger Δf shift of −44 Hz occurred for denatured BSA oligomers (Figure 4a). The corresponding ΔD shifts were around 4×10^{-6} and 5×10^{-6} for native BSA and denatured BSA, respectively (Figure 4b). The combination of Δf and ΔD shifts is indicative of greater mass uptake of denatured BSA. After saturation, a buffer washing step was performed and caused a decrease in the magnitude of the Δf shifts until reaching stable values of −26 and −38 Hz for native and denatured BSA, respectively. The corresponding ΔD shifts were around 2×10^{-6} and 2.5×10^{-6} for native and denatured BSA, respectively. Hence, the findings support that there is a larger adsorption uptake of denatured BSA oligomers than native BSA monomers.

Of particular note, it was observed that the adsorption time scale to reach saturation (initial uptake) was significantly shorter for denatured BSA oligomers compared to native BSA monomers, implying that denatured BSA might require shorter coating times for effectiveness. This trend was noteworthy because BSA protein adsorption is a diffusion-limited process[53] and larger denatured BSA oligomers would have a smaller diffusion coefficient in bulk solution than native BSA monomers. As such, one might initially expect that the

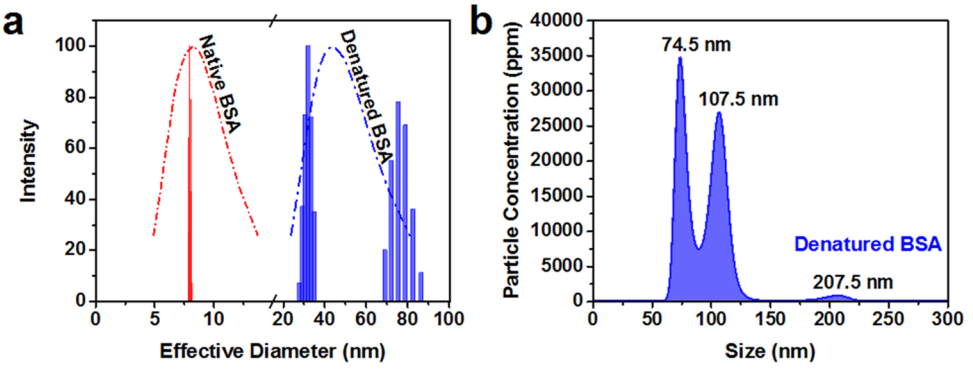

Figure 3. DLS and NTA measurements of BSA protein size distribution. (a) Intensity-weighted size distribution of native and denatured BSA is reported from DLS measurements. (b) Number-weighted size distribution of denatured BSA is reported from NTA measurements.

DOI: 10.1021/acsami.8b13749
ACS Appl. Mater. Interfaces 2018, 10, 32047−32057

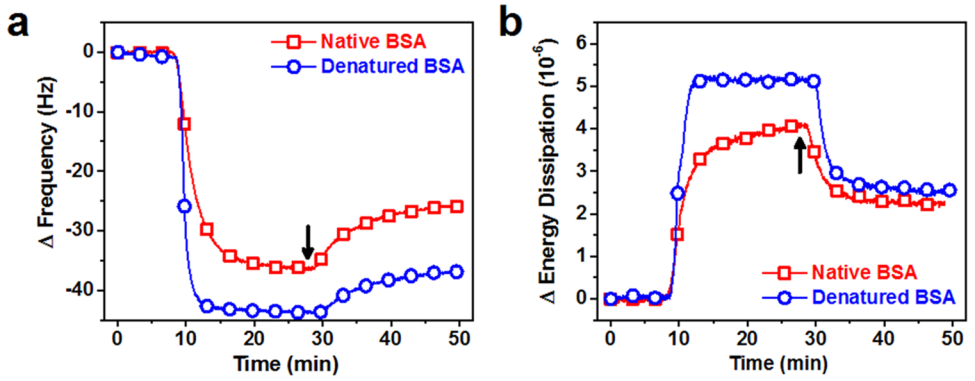

Figure 4. QCM-D measurements of native and denatured BSA protein adsorption onto silica surfaces. Changes in (a) resonance frequency and (b) energy dissipation were recorded as a function of time. A baseline was established in buffer solution before 100 μM BSA was injected under continuous flow conditions at around t = 8 min. After the adsorption process reached saturation, a buffer washing step was performed (see arrows).

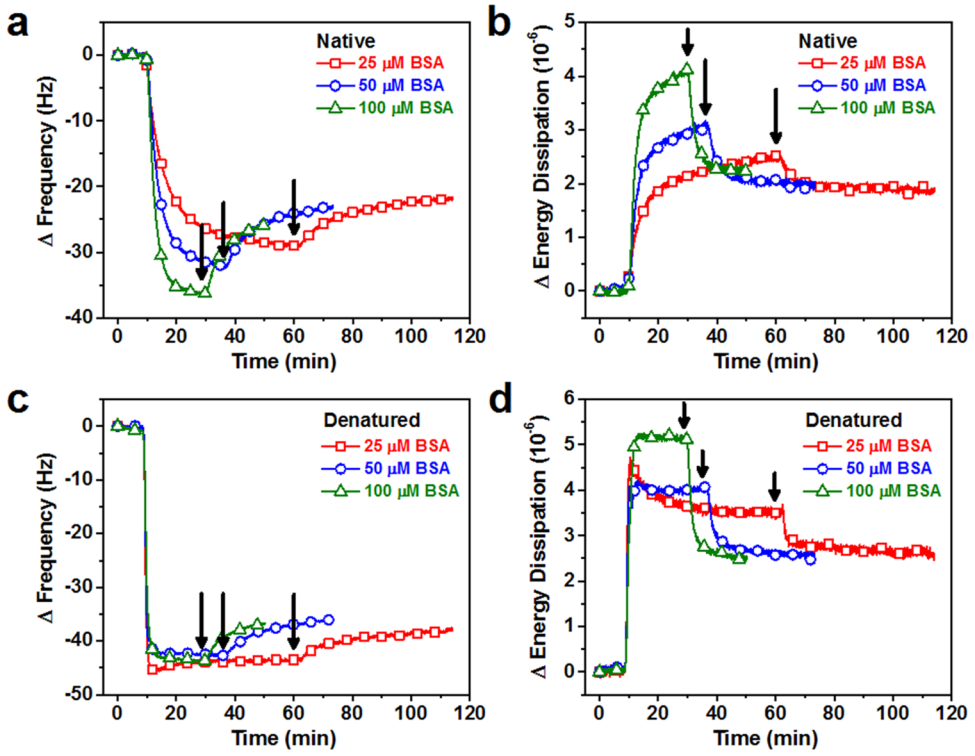

Figure 5. QCM-D measurements of concentration-dependent native and denatured BSA protein adsorption onto silica surfaces. Changes in (a) resonance frequency and (b) energy dissipation were recorded as a function of time for native BSA at different protein concentrations. (c, d) Corresponding measurement responses for denatured BSA. A baseline was established in buffer solution before BSA was injected under continuous flow conditions at around t = 8 min. After the adsorption process reached saturation, a buffer washing step was performed (see arrows).

diffusion-limited adsorption rate of denatured BSA would be slower than that of native BSA. To explain our experimental observation that the apparent adsorption rate of denatured BSA is in fact greater, it should be noted that native BSA monomers weakly attach to silica surfaces,[15] and hence the ensemble-average measurement response tracked by QCM-D measurements reflects the net rate of adsorption and desorption of BSA protein molecules.[54] Previously, Kwok et al. reported that 99.3% of attaching (native) BSA monomers desorb from the silica surface.[15] As such, the greater rate of change in the QCM-D measurement responses for denatured BSA oligomers indicates that the rate of desorption is lower for denatured BSA oligomers than for native BSA monomers.

This finding is supported by several related factors. First, the larger oligomers of predenatured BSA molecules would have a greater contacting surface area per adsorbing species, resulting in a stronger net interaction. Second, the two-dimensional Brownian motion exerted on larger BSA oligomers is also lower, and hence the likelihood of desorption promoted by lateral forces is lower as well. The two points are supported by the work of Schwartz and colleagues,[55] in which the adsorption of monomeric and oligomeric fibrinogen was studied. The authors proposed that favorable orientations for protein adsorption were more likely to occur for oligomers on account of their larger size, and slower diffusion at the surface would lead to less desorption. In comparison to native BSA monomers, attenuated total reflectance Fourier transform infrared (ATR-FTIR) spectroscopic experiments also revealed that the heat-pretreated, denatured BSA oligomers undergo a relatively low degree of additional, surface-induced conforma-

DOI: 10.1021/acsami.8b13749
ACS Appl. Mater. Interfaces 2018, 10, 32047−32057

tional changes in the adsorbed state (Figure S1 and Table S1). Taken together, the findings support that denatured BSA oligomers adhere more strongly onto silica surfaces than native BSA monomers because denatured BSA oligomers have altered conformational properties and greater surface contact area per adsorbing species. This combination of features results in greater adsorption uptake and a shorter time required for coating denatured BSA on silica surfaces.

Effect of BSA Concentration on QCM-D Adsorption Kinetics. We next tested whether native and denatured BSA exhibited similar patterns of adsorption across a broader range of bulk protein concentrations (Figure 5). For native BSA, the adsorption kinetics and corresponding uptake depended on the protein concentration (Figure 5a,b). For 25 μM BSA, it took nearly 1 h to reach saturation. The observed trends are consistent with past observations,[22,56−58] and reinforce that high protein concentrations and long incubation times are required to coat silica surfaces with native BSA. In marked contrast, for denatured BSA, the adsorption kinetics and the corresponding uptakes were largely independent of protein concentration (Figure 5c,d). Importantly, rapid uptake was observed for denatured BSA oligomers at all tested concentrations, demonstrating that the coating approach is versatile and superior to using native BSA monomers.

The thickness of the BSA protein adlayers was also estimated by applying the Voigt−Voinova model to analyze the QCM-D measurement data (Table 1).[59] In general, the modeling results support that denatured BSA oligomers formed thicker adlayers than native BSA monomers, and this trend was consistent across the tested protein concentrations. Of note, for each type of BSA protein, the estimated thickness of the protein adlayers at saturation was greatest for the highest bulk protein concentration (100 μM). This concentration-dependent effect can be attributed to rapid uptake before the adsorbed protein molecules assume an optimal packing state.[60] Indeed, upon buffer washing, the adsorbed molecules reorganized such that the adlayer thicknesses were similar across the tested protein concentrations and resulted in stable protein coatings. Overall, the observed trends were also supported by atomic force microscopy (AFM) experiments, indicating that denatured BSA oligomers formed denser, thicker adlayers than native BSA monomers (Figure S2).

Table 1. Effective Mass and Thickness of Adsorbed Native and Denatured BSA Layers[a]

BSA concentration and type	acoustic mass (ng cm^{-2})	thickness at Saturation (nm)	acoustic mass (ng cm^{-2})	thickness after rinsing (nm)
25 μM native	663	5.1	494	3.8
50 μM native	754	5.8	507	3.9
100 μM native	897	6.9	546	4.2
25 μM denatured	1053	8.1	832	6.4
50 μM denatured	1079	8.3	754	5.8
100 μM denatured	1495	11.5	806	6.2

[a]Voigt−Voinova modeling was performed on QCM-D measurement data from Figure 5.

LSPR Measurements on Native and Denatured BSA Adsorption. To verify the trend in adsorption kinetics, ensemble-average LSPR measurements were performed to track native and denatured BSA adsorption onto silica-coated gold nanodisk arrays (Figure S3). While QCM-D measurements are sensitive to bound protein mass and hydrodynamic-coupled solvent, LSPR measurements are sensitive only to bound protein and hence provide a more direct evaluation of protein adsorption.[61−63] LSPR measurements are also highly surface-sensitive with a small probing volume that is suitable for detecting conformational changes in adsorbed protein molecules.[64,65] In particular, there is a sharp decay in the evanescent electromagnetic field intensity emanating from the sensor surface and this high measurement sensitivity can be used to detect changes in structural configuration of adsorbed molecules.[36,61,66,67]

The LSPR measurement trends for both native and denatured BSA adsorption showed excellent agreement with the QCM-D measurements. For native BSA monomers, the recorded final peak shifts were 0.76, 0.61, and 0.49 nm for 100, 50, and 25 μM protein concentrations, respectively (Figure 6a). The magnitude of the peak shift for 100 μM native BSA agreed well with previous measurements,[28] while the concentration-dependent trend in measurement responses is consistent with diffusion-limited adsorption kinetics. On the other hand, denatured BSA oligomers exhibited rapid adsorption kinetics for all tested concentrations, reaching saturation on similar time scales and the final peak shifts were between 0.9 and 1.0 nm (Figure 6b). Comparatively, the results further support that there is a greater uptake of bound protein for denatured BSA and the corresponding adsorption kinetics are quicker. These findings are consistent with a thicker and/or denser layer of denatured BSA on the sensor surface.

Upon a buffer washing step, there was a transient increase in the LSPR peak shift for denatured BSA, followed by a gradual decrease in peak shift until reaching a stabilized value. The magnitude of the transient spike correlated with the bulk protein concentration that was used for coating, and is likely due to a structural rearrangement among bound BSA molecules in the adlayer, whereby some molecules become closer to the silica surface while other protein molecules desorb.[68,69] Of note, the final peak shifts after washing were nearly identical for all native BSA samples and likewise for all denatured BSA samples. Hence, the LSPR measurements provided confirmatory evidence that a larger amount of denatured BSA oligomers adsorbs on silica and the adsorption process is quicker, compared to native BSA monomers. Also, similar results were obtained across tested protein concentrations, supporting that denatured BSA oligomers provide a robust and versatile option for surface passivation.

Evaluation of Blocking Efficiency against Serum Biofouling. On the basis of the improved adsorption properties of denatured BSA, we next tested the blocking efficiency of native and denatured BSA surface coatings to inhibit biofouling of silica surfaces upon contact with whole fetal bovine serum (FBS) (Figure 7a). The degree of blocking efficiency was assessed by QCM-D experiments, whereby the extent to which BSA coatings inhibited fouling by serum components was determined relative to control experiments conducted with bare silica surfaces (Figure 7b).[36] Briefly, a measurement baseline was established in Tris buffer solution, followed by the addition of either 100 μM native or denatured BSA for 3 min, 30 min, or 3 h incubation periods before a buffer washing step. Weakly adsorbed protein molecules were removed during the washing step, while the remaining

DOI: 10.1021/acsami.8b13749
ACS Appl. Mater. Interfaces 2018, 10, 32047−32057

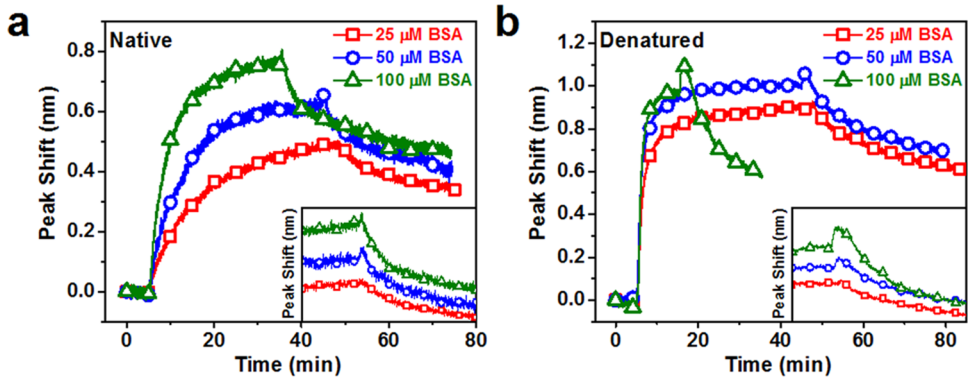

Figure 6. LSPR measurements of concentration-dependent native and denatured BSA protein adsorption onto silica-coated gold nanodisk arrays. Wavelength-shift LSPR measurements were recorded for (a) native and (b) denatured BSA protein adsorption onto silica-coated gold nanodisk arrays. The LSPR peak shift was recorded as a function of time. A baseline was established in buffer solution before BSA was injected under continuous flow conditions at around t = 5 min. After the adsorption process reached saturation, a buffer washing step was performed (see arrows). The curves in the insets are superimposed such that the washing step occurs at the same time point for direct comparison.

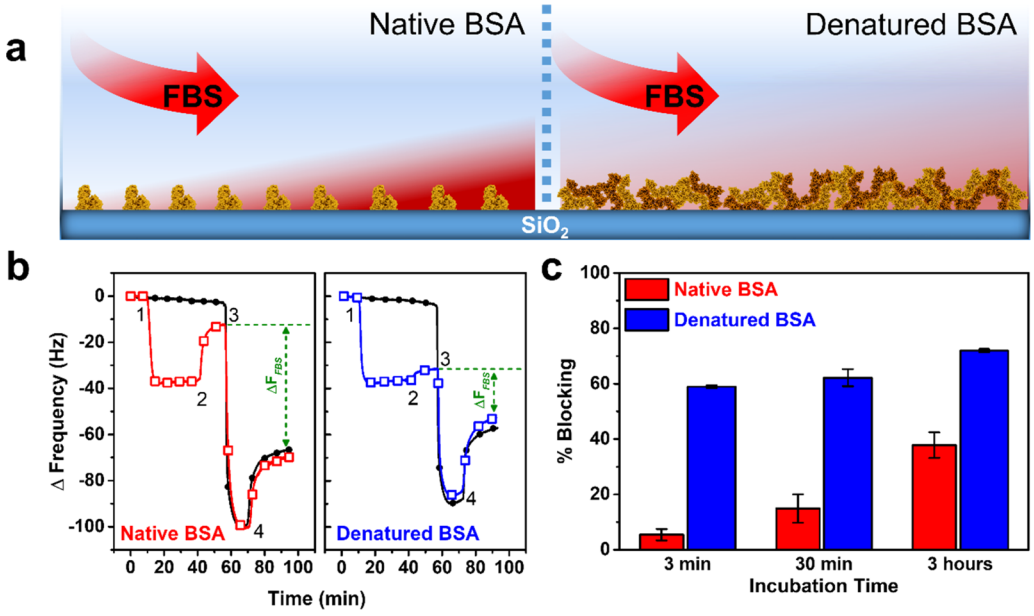

Figure 7. Blocking efficiency of adsorbed native and denatured BSA protein layers in response to biofouling. (a) Schematic illustration of protein-based passivation coatings composed of native or denatured BSA molecules. (b) Change in QCM-D Δf shifts as a function of time to determine blocking efficiency of native and denatured BSA coatings. The measurement baselines were recorded in Tris buffer solution and then (1) 100 μM BSA was added to Tris buffer, (2) rinsed with Tris buffer, (3) injected with 100% FBS, and (4) rinsed with Tris buffer. A control experiment without BSA coating was run on a bare silica surface. The final Δf shift relative to the protein coating step was assigned as a measure of biofouling, and the percentage of blocking efficiency was calculated in comparison to biofouling on the bare silica control. (c) Blocking efficiency of native and denatured BSA protein layers as a function of incubation time during coating process. The red and blue columns refer to native and denatured BSA, respectively. Data are expressed as mean ± standard deviation for n = 3 measurements.

adsorbed protein molecules were strongly bound, thus minimizing possible Vroman effects.[70−72] Then, 100% FBS was incubated in the measurement chamber, followed by a buffer washing step. The blocking efficiency was determined by comparing the final Δf shifts in buffer solution after FBS incubation to those of a control experiment in which BSA was not injected. While BSA passivation typically involves a 1 h or longer incubation step, the different incubation times were tested to determine if denatured BSA could streamline the coating time while improving blocking efficiency as well.

After a conventional 3 h incubation time, the blocking efficiency of denatured BSA was 72.9 ± 0.5%, while the blocking efficiency of native BSA was only 37.8 ± 4.6% (Figure 7c). For 30 min incubation, the difference in blocking efficiencies was even larger, and the values for denatured and native BSA were 62.2 ± 3.1 and 14.9 ± 5.1%, respectively. When the incubation time was reduced to 3 min, denatured BSA still had a high blocking efficiency of 58.9 ± 0.5%, whereas the efficiency of native BSA was reduced to 5.5 ± 2.1%—greater than 10-fold difference in blocking efficiencies. Of particular note, the blocking efficiency of denatured BSA with 3 min incubation was superior to native BSA even after 3 h incubation. This finding is consistent with the aforementioned characterization results, indicating that denatured BSA oligomers form a denser and thicker adlayer. Taken together, our results demonstrate how purposefully modulating the structural and conformational properties of BSA protein in

DOI: 10.1021/acsami.8b13749
ACS Appl. Mater. Interfaces 2018, 10, 32047−32057

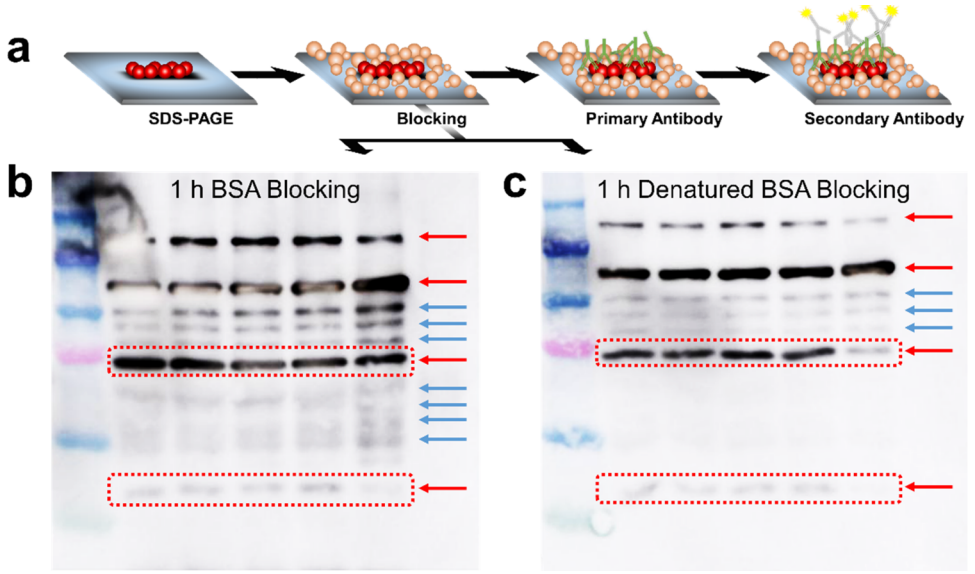

Figure 8. SDS-PAGE/Western blot analysis for performance comparison of native BSA monomers and predenatured BSA oligomers as blocking agents. (a) Schematic illustration of step-by-step protocol using either native BSA monomers or predenatured BSA oligomers as a blocking agent. Each gel was loaded with silica nanoparticle-treated serum (lanes 1−4), untreated serum (lane 5), and a blank with buffer only (lane 6). The gels were blocked with (b) native BSA monomers or (c) predenatured BSA oligomers prior to antibody incubation. The bands corresponding to protein biomarkers and nonspecific bands are indicated by the red and blue arrows, respectively. The boxes show differences in band intensity, indicating the superior performance of denatured BSA oligomers.

bulk solution can lead to improved protein coatings for surface passivation applications.

Western Blot Application. We further investigated the application performance of using denatured BSA oligomers instead of native BSA monomers as a blocking agent in Western blot analysis, which is a widely used immunochemical assay for semiquantitative detection of proteins. As presented in Figure 8a, the procedure consists of a gel electrophoresis step to separate individual proteins by molecular size, followed by electrophoretic transfer of the proteins to a nitrocellulose membrane. The target protein(s) is detected by immunostaining with primary and secondary antibodies; the primary antibody recognizes and binds selectively to the target protein while the secondary antibody binds selectively to the primary antibody and provides some type of chemical or fluorescent readout. Prior to immunostaining, a blocking step is required to minimize nonspecific attachment of antibodies to the membrane or other biological materials. These nonspecific events can yield false signals and hence milk (which contains proteins) or 3−5% native BSA monomers are commonly used as a blocking agent. In short, the blocking agent is incubated with the membrane prior to antibody addition.

On the basis of this approach, we investigated the immune reaction of human blood serum exposed to bare silica nanoparticles and measured the levels of C3b and iC3b protein biomarkers, which indicate activation of the complement system. Briefly, 1% normal human serum samples were incubated with or without silica nanoparticles for 30 min at 37 °C and the supernatants were loaded for analysis in the following order: nanoparticle-treated serum (lanes 1−4), untreated serum (lane 5), and buffer blank (lane 6). The membranes were blocked for an hour with a buffer solution containing either 3% native BSA monomers or 3% predenatured BSA oligomers (Figure 8b,c). After immunostaining, it was possible to detect bands corresponding to C3b protein (∼175 and ∼104 kDa) and iC3b protein (∼63 and ∼42 kDa) (see red arrows).[73] Nonspecific antibody binding was detected at other bands as well. Importantly, the number and intensity of nonspecific bands were reduced significantly when using predenatured BSA oligomers, in marked contrast to native BSA monomers (see blue arrows). Indeed, predenatured BSA oligomers also minimized nonspecific iC3b band intensity in the untreated serum control to a greater extent than native BSA monomers. Hence, predenatured BSA oligomers demonstrated superior performance as a blocking agent for Western blot applications.

CONCLUSIONS

In this work, we have established a simple and versatile method to increase the stickiness of BSA adsorption onto silica surfaces, which led to improved surface passivation and shorter coating times. The underlying concept is based on utilizing thermal denaturation to purposefully modulate the structural and conformational properties of BSA molecules in bulk solution to promote greater adsorption uptake and more irreversible adsorption. These findings build on growing fundamental knowledge about how the structural and conformational properties of a protein in bulk solution influence protein adsorption, while presenting the first example of how this fundamental knowledge can be translated into a functional application with high performance. Given the wide usage of BSA as a surface-passivating agent and simple method to convert native BSA monomers into denatured BSA oligomers, there are broad possibilities for utilizing denatured BSA in various application settings and for preparing improved protein-based coatings.

ASSOCIATED CONTENT

Supporting Information

The Supporting Information is available free of charge on the ACS Publications website at DOI: 10.1021/acsami.8b13749.

DOI: 10.1021/acsami.8b13749
ACS Appl. Mater. Interfaces 2018, 10, 32047−32057

Additional data are provided for details of CD spectroscopy data analysis; ATR-FTIR spectroscopic characterization of BSA protein adlayers (Figure S1 and Table S1); AFM characterization of BSA protein adlayers (Figure S2); and scanning electron microscopy characterization of LSPR measurement platform (Figure S3) (PDF)

AUTHOR INFORMATION

Corresponding Author

*E-mail: njcho@ntu.edu.sg.

ORCID

Joshua A. Jackman: 0000-0002-1800-8102

Nam-Joon Cho: 0000-0002-8692-8955

Notes

The authors declare no competing financial interest.

ACKNOWLEDGMENTS

This work was supported by the National Research Foundation of Singapore through a Competitive Research Programme grant (NRF-CRP10-2012-07) and a Proof-of-Concept grant (NRF2015NRF-POC0001-19) as well as through the Center for Precision Biology at Nanyang Technological University. Additional support was provided by the Creative Materials Discovery Program through the National Research Foundation of Korea funded by the Ministry of Science, ICT and Future Planning (NRF-2016M3D1A1024098). The authors thank E. Linardy for technical assistance with experiments.

REFERENCES

(1) Nakanishi, K.; Sakiyama, T.; Imamura, K. On the Adsorption of Proteins on Solid Surfaces, A Common but Very Complicated Phenomenon. *J. Biosci. Bioeng.* **2001**, *91*, 233−244.

(2) Gray, J. J. The Interaction of Proteins With Solid Surfaces. *Curr. Opin. Struct. Biol.* **2004**, *14*, 110−115.

(3) Rabe, M.; Verdes, D.; Seeger, S. Understanding Protein Adsorption Phenomena at Solid Surfaces. *Adv. Colloid Interface Sci.* **2011**, *162*, 87−106.

(4) Emilsson, G.; Schoch, R. L.; Feuz, L.; Höök, F.; Lim, R. Y.; Dahlin, A. B. Strongly Stretched Protein Resistant Poly(Ethylene Glycol) Brushes Prepared by Grafting-To. *ACS Appl. Mater. Interfaces* **2015**, *7*, 7505−7515.

(5) Yu, L.; Cheng, C.; Ran, Q.; Schlaich, C.; Noeske, P.-L. M.; Li, W.; Wei, Q.; Haag, R. Bioinspired Universal Monolayer Coatings by Combining Concepts from Blood Protein Adsorption and Mussel Adhesion. *ACS Appl. Mater. Interfaces* **2017**, *9*, 6624−6633.

(6) Yu, L.; Hou, Y.; Cheng, C.; Schlaich, C.; Noeske, P.-L. M.; Wei, Q.; Haag, R. High-Antifouling Polymer Brush Coatings on Nonpolar Surfaces via Adsorption-Crosslinking Strategy. *ACS Appl. Mater. Interfaces* **2017**, 44281−44292.

(7) Bog, U.; de los Santos Pereira, A.; Mueller, S. L.; Havenridge, S.; Parrillo, V.; Bruns, M.; Holmes, A. E.; Rodriguez-Emmenegger, C.; Fuchs, H.; Hirtz, M. Clickable Antifouling Polymer Brushes for Polymer Pen Lithography. *ACS Appl. Mater. Interfaces* **2017**, *9*, 12109−12117.

(8) Wei, Q.; Becherer, T.; Angioletti-Uberti, S.; Dzubiella, J.; Wischke, C.; Neffe, A. T.; Lendlein, A.; Ballauff, M.; Haag, R. Protein Interactions with Polymer Coatings and Biomaterials. *Angew. Chem., Int. Ed.* **2014**, *53*, 8004−8031.

(9) Wei, Q.; Haag, R. Universal Polymer Coatings and their Representative Biomedical Applications. *Mater. Horiz.* **2015**, *2*, 567−577.

(10) Steinitz, M. Quantitation of the Blocking Effect of Tween 20 and Bovine Serum Albumin in ELISA Microwells. *Anal. Biochem.* **2000**, *282*, 232−238.

(11) Gibbs, J. *Effective Blocking Procedures*; ELISA Technical Bulletin No 3; Corning Incorporated: Corning, New York., 2001; pp 1−6.

(12) Sweryda-Krawiec, B.; Devaraj, H.; Jacob, G.; Hickman, J. J. A New Interpretation of Serum Albumin Surface Passivation. *Langmuir* **2004**, *20*, 2054−2056.

(13) Fang, B.; Ling, Q.; Zhao, W.; Ma, Y.; Bai, P.; Wei, Q.; Li, H.; Zhao, C. Modification of Polyethersulfone Membrane by Grafting Bovine Serum Albumin on the Surface of Polyethersulfone/Poly-(Acrylonitrile-co-Acrylic Acid) Blended Membrane. *J. Membr. Sci.* **2009**, *329*, 46−55.

(14) Wei, Q.; Li, B.; Yi, N.; Su, B.; Yin, Z.; Zhang, F.; Li, J.; Zhao, C. Improving the Blood Compatibility of Material Surfaces via Biomolecule-Immobilized Mussel-Inspired Coatings. *J. Biomed. Mater. Res., Part A* **2011**, *96*, 38−45.

(15) Kwok, K. C.; Yeung, K. M.; Cheung, N. H. Adsorption Kinetics of Bovine Serum Albumin on Fused Silica: Population Heterogeneities Revealed by Single-Molecule Fluorescence Microscopy. *Langmuir* **2007**, *23*, 1948−1952.

(16) Yoshikawa, C.; Goto, A.; Tsujii, Y.; Fukuda, T.; Kimura, T.; Yamamoto, K.; Kishida, A. Protein Repellency of Well-Defined, Concentrated Poly(2-Hydroxyethyl Methacrylate) Brushes by the Size-Exclusion Effect. *Macromolecules* **2006**, *39*, 2284−2290.

(17) Jeyachandran, Y. L.; Mielczarski, E.; Rai, B.; Mielczarski, J. A. Quantitative and Qualitative Evaluation of Adsorption/Desorption of Bovine Serum Albumin on Hydrophilic and Hydrophobic Surfaces. *Langmuir* **2009**, *25*, 11614−11620.

(18) Penna, M. J.; Mijajlovic, M.; Biggs, M. J. Molecular-Level Understanding of Protein Adsorption at the Interface between Water and a Strongly Interacting Uncharged Solid Surface. *J. Am. Chem. Soc.* **2014**, *136*, 5323−5331.

(19) Santore, M. M.; Wertz, C. F. Protein Spreading Kinetics at Liquid−Solid Interfaces via an Adsorption Probe Method. *Langmuir* **2005**, *21*, 10172−10178.

(20) Calonder, C.; Tie, Y.; Van Tassel, P. R. History Dependence of Protein Adsorption Kinetics. *Proc. Natl. Acad. Sci. U.S.A.* **2001**, *98*, 10664.

(21) Tsapikouni, T. S.; Missirlis, Y. F. Protein−Material Interactions: From Micro-to-Nano Scale. *Mater. Sci. Eng., B* **2008**, *152*, 2−7.

(22) Giacomelli, C. E.; Norde, W. The Adsorption−Desorption Cycle. Reversibility of the BSA−Silica System. *J. Colloid Interface Sci.* **2001**, *233*, 234−240.

(23) Karlsson, M.; Ekeroth, J.; Elwing, H.; Carlsson, U. Reduction of Irreversible Protein Adsorption on Solid Surfaces by Protein Engineering for Increased Stability. *J. Biol. Chem.* **2005**, *280*, 25558−25564.

(24) Goli, K. K.; Rojas, O. J.; Özçam, A. E.; Genzer, J. Generation of Functional Coatings on Hydrophobic Surfaces Through Deposition of Denatured Proteins Followed by Grafting from Polymerization. *Biomacromolecules* **2012**, *13*, 1371−1382.

(25) Goli, K. K.; Rojas, O. J.; Genzer, J. Formation and Antifouling Properties of Amphiphilic Coatings on Polypropylene Fibers. *Biomacromolecules* **2012**, *13*, 3769−3779.

(26) Damodaran, S.; Song, K. B. Kinetics of Adsorption of Proteins at Interfaces: Role of Protein Conformation in Diffusional Adsorption. *Biochim. Biophys. Acta, Protein Struct. Mol. Enzymol.* **1988**, *954*, 253−264.

(27) Shirahama, H.; Suzawa, T. Adsorption of Heat-Denatured Albumin onto Polymer Latices. *J. Colloid Interface Sci.* **1988**, *126*, 269−277.

(28) Jackman, J. A.; Ferhan, A. R.; Yoon, B. K.; Park, J. H.; Zhdanov, V. P.; Cho, N.-J. Indirect Nanoplasmonic Sensing Platform for Monitoring Temperature-Dependent Protein Adsorption. *Anal. Chem.* **2017**, *89*, 12976−12983.

(29) Wang, Q.; Kuo, Y.; Wang, Y.; Shin, G.; Ruengruglikit, C.; Huang, Q. Luminescent Properties of Water-Soluble Denatured

DOI: 10.1021/acsami.8b13749
ACS Appl. Mater. Interfaces 2018, 10, 32047−32057

Bovine Serum Albumin-Coated CdTe Quantum Dots. *J. Phys. Chem. B* **2006**, *110*, 16860−16866.
(30) Zhang, M.; Cao, Y.; Wang, L.; Ma, Y.; Tu, X.; Zhang, Z. Manganese Doped Iron Oxide Theranostic Nanoparticles for Combined T_1 Magnetic Resonance Imaging and Photothermal Therapy. *ACS Appl. Mater. Interfaces* **2015**, *7*, 4650−4658.
(31) Kim, K. S.; Um, Y. M.; Jang, J.-r.; Choe, W.-S.; Yoo, P. J. Highly Sensitive Reduced Graphene Oxide Impedance Sensor Harnessing π-Stacking Interaction Mediated Direct Deposition of Protein Probes. *ACS Appl. Mater. Interfaces* **2013**, *5*, 3591−3598.
(32) Jang, S. K.; Jang, J.-r.; Choe, W.-S.; Lee, S. Harnessing Denatured Protein for Controllable Bipolar Doping of a Monolayer Graphene. *ACS Appl. Mater. Interfaces* **2015**, *7*, 1250−1256.
(33) Zhou, L.; Wang, K.; Wu, Z.; Dong, H.; Sun, H.; Cheng, X.; Zhang, H. l.; Zhou, H.; Jia, C.; Jin, Q.; Mao, H.; Coll, J.-L.; Zhao, J. Investigation of Controllable Nanoscale Heat-Denatured Bovine Serum Albumin Films on Graphene. *Langmuir* **2016**, *32*, 12623−12631.
(34) Bakshi, M. S.; Thakur, P.; Kaur, G.; Kaur, H.; Banipal, T. S.; Possmayer, F.; Petersen, N. O. Stabilization of PbS Nanocrystals by Bovine Serum Albumin in its Native and Denatured States. *Adv. Funct. Mater.* **2009**, *19*, 1451−1458.
(35) Bu, X.; Zhou, Y.; He, M.; Chen, Z.; Zhang, T. Bioinspired, Direct Synthesis of Aqueous CdSe Quantum Dots for High-Sensitive Copper (II) Ion Detection. *Dalton Trans.* **2013**, *42*, 15411−15420.
(36) Park, J. H.; Sut, T. N.; Jackman, J. A.; Ferhan, A. R.; Yoon, B. K.; Cho, N.-J. Controlling Adsorption and Passivation Properties of Bovine Serum Albumin on Silica Surfaces by Ionic Strength Modulation and Cross-Linking. *Phys. Chem. Chem. Phys.* **2017**, *19*, 8854−8865.
(37) Cho, N.-J.; Frank, C. W.; Kasemo, B.; Höök, F. Quartz Crystal Microbalance with Dissipation Monitoring of Supported Lipid Bilayers on Various Substrates. *Nat. Protoc.* **2010**, *5*, 1096−1106.
(38) Voinova, M. V.; Jonson, M.; Kasemo, B. 'Missing Mass' Effect in Biosensor's QCM Applications. *Biosens. Bioelectron.* **2002**, *17*, 835−841.
(39) Jackman, J. A.; Zhdanov, V. P.; Cho, N.-J. Nanoplasmonic Biosensing for Soft Matter Adsorption: Kinetics of Lipid Vesicle Attachment and Shape Deformation. *Langmuir* **2014**, *30*, 9494−9503.
(40) Fredriksson, H.; Alaverdyan, Y.; Dmitriev, A.; Langhammer, C.; Sutherland, D. S.; Zäch, M.; Kasemo, B. Hole−Mask Colloidal Lithography. *Adv. Mater.* **2007**, *19*, 4297−4302.
(41) Dahlin, A. B.; Tegenfeldt, J. O.; Höök, F. Improving the Instrumental Resolution of Sensors Based on Localized Surface Plasmon Resonance. *Anal. Chem.* **2006**, *78*, 4416−4423.
(42) Murayama, K.; Tomida, M. Heat-Induced Secondary Structure and Conformation Change of Bovine Serum Albumin Investigated by Fourier Transform Infrared Spectroscopy. *Biochemistry* **2004**, *43*, 11526−11532.
(43) Takeda, K.; Wada, A.; Yamamoto, K.; Moriyama, Y.; Aoki, K. Conformational Change of Bovine Serum Albumin by Heat Treatment. *J. Protein Chem.* **1989**, *8*, 653−659.
(44) Moriyama, Y.; Kawasaka, Y.; Takeda, K. Protective Effect of Small Amounts of Sodium Dodecyl Sulfate on the Helical Structure of Bovine Serum Albumin in Thermal Denaturation. *J. Colloid Interface Sci.* **2003**, *257*, 41−46.
(45) Moriyama, Y.; Watanabe, E.; Kobayashi, K.; Harano, H.; Inui, E.; Takeda, K. Secondary Structural Change of Bovine Serum Albumin in Thermal Denaturation up to 130 C and Protective Effect of Sodium Dodecyl Sulfate on the Change. *J. Phys. Chem. B* **2008**, *112*, 16585−16589.
(46) Militello, V.; Casarino, C.; Emanuele, A.; Giostra, A.; Pullara, F.; Leone, M. Aggregation Kinetics of Bovine Serum Albumin Studied by FTIR Spectroscopy and Light Scattering. *Biophys. Chem.* **2004**, *107*, 175−187.
(47) Chi, E. Y.; Krishnan, S.; Randolph, T. W.; Carpenter, J. F. Physical Stability of Proteins in Aqueous Solution: Mechanism and Driving Forces in Nonnative Protein Aggregation. *Pharm. Res.* **2003**, *20*, 1325−1336.
(48) Dobson, C. M. Principles of Protein Folding, Misfolding and Aggregation. *Semin. Cell Dev. Biol.* **2004**, *15*, 3−16.
(49) Philo, J. S.; Arakawa, T. Mechanisms of Protein Aggregation. *Curr. Pharm. Biotechnol.* **2009**, *10*, 348−351.
(50) Norde, W. Driving Forces for Protein Adsorption at Solid Surfaces. *Macromol. Symp.* **1996**, 5−18.
(51) Kurrat, R.; Prenosil, J. E.; Ramsden, J. J. Kinetics of Human and Bovine Serum Albumin Adsorption at Silica−Titania Surfaces. *J. Colloid Interface Sci.* **1997**, *185*, 1−8.
(52) Jeyachandran, Y. L.; Mielczarski, J. A.; Mielczarski, E.; Rai, B. Efficiency of Blocking of Non-Specific Interaction of Different Proteins by BSA Adsorbed on Hydrophobic and Hydrophilic Surfaces. *J. Colloid Interface Sci.* **2010**, *341*, 136−142.
(53) Zhdanov, V.; Kasemo, B. Monte Carlo Simulation of the Kinetics of Protein Adsorption. *Proteins: Struct., Funct., Bioinf.* **1998**, *30*, 177−182.
(54) Hain, N.; Gallego, M.; Reviakine, I. Unraveling Supported Lipid Bilayer Formation Kinetics: Osmotic Effects. *Langmuir* **2013**, *29*, 2282−2288.
(55) Kastantin, M.; Langdon, B. B.; Chang, E. L.; Schwartz, D. K. Single-Molecule Resolution of Interfacial Fibrinogen Behavior: Effects of Oligomer Populations and Surface Chemistry. *J. Am. Chem. Soc.* **2011**, *133*, 4975−4983.
(56) Roach, P.; Farrar, D.; Perry, C. C. Interpretation of Protein Adsorption: Surface-Induced Conformational Changes. *J. Am. Chem. Soc.* **2005**, *127*, 8168−8173.
(57) McClellan, S. J.; Franses, E. I. Adsorption of Bovine Serum Albumin at Solid/Aqueous Interfaces. *Colloids Surf., A* **2005**, *260*, 265−275.
(58) McClellan, S. J.; Franses, E. I. Effect of Concentration and Denaturation on Adsorption and Surface Tension of Bovine Serum Albumin. *Colloids Surf., B* **2003**, *28*, 63−75.
(59) Voinova, M. V.; Rodahl, M.; Jonson, M.; Kasemo, B. Viscoelastic Acoustic Response of Layered Polymer Films at Fluid-Solid Interfaces: Continuum Mechanics Approach. *Phys. Scr.* **1999**, *59*, 391.
(60) Ramsden, J. Puzzles and Paradoxes in Protein Adsorption. *Chem. Soc. Rev.* **1995**, *24*, 73−78.
(61) Jackman, J. A.; Avsar, S. Y.; Ferhan, A. R.; Li, D.; Park, J. H.; Zhdanov, V. P.; Cho, N.-J. Quantitative Profiling of Nanoscale Liposome Deformation by a Localized Surface Plasmon Resonance Sensor. *Anal. Chem.* **2017**, *89*, 1102−1109.
(62) Ferhan, A. R.; Jackman, J. A.; Cho, N.-J. Investigating How Vesicle Size Influences Vesicle Adsorption on Titanium Oxide: A Competition Between Steric Packing and Shape Deformation. *Phys. Chem. Chem. Phys.* **2017**, *19*, 2131−2139.
(63) Ferhan, A. R.; Jackman, J. A.; Cho, N.-J. Probing Spatial Proximity of Supported Lipid Bilayers to Silica Surfaces by Localized Surface Plasmon Resonance Sensing. *Anal. Chem.* **2017**, *89*, 4301−4308.
(64) Hall, W. P.; Anker, J. N.; Lin, Y.; Modica, J.; Mrksich, M.; Van Duyne, R. P. A Calcium-Modulated Plasmonic Switch. *J. Am. Chem. Soc.* **2008**, *130*, 5836−5837.
(65) Hall, W. P.; Modica, J.; Anker, J.; Lin, Y.; Mrksich, M.; Van Duyne, R. P. A Conformation- and Ion-Sensitive Plasmonic Biosensor. *Nano Lett.* **2011**, *11*, 1098−1105.
(66) Oh, E.; Jackman, J. A.; Yorulmaz, S.; Zhdanov, V. P.; Lee, H.; Cho, N.-J. Contribution of Temperature to Deformation of Adsorbed Vesicles Studied by Nanoplasmonic Biosensing. *Langmuir* **2015**, *31*, 771−781.
(67) Dacic, M.; Jackman, J. A.; Yorulmaz, S.; Zhdanov, V. P.; Kasemo, B.; Cho, N.-J. Influence of Divalent Cations on Deformation and Rupture of Adsorbed Lipid Vesicles. *Langmuir* **2016**, *32*, 6486−6495.
(68) Daly, S. M.; Przybycien, T. M.; Tilton, R. D. Coverage-dependent Orientation of Lysozyme Adsorbed on Silica. *Langmuir* **2003**, *19*, 3848−3857.

DOI: 10.1021/acsami.8b13749
ACS Appl. Mater. Interfaces 2018, 10, 32047−32057

(69) Wertz, C. F.; Santore, M. M. Adsorption and Reorientation Kinetics of Lysozyme on Hydrophobic Surfaces. *Langmuir* **2002**, *18*, 1190−1199.
(70) Jung, S.-Y.; Lim, S.-M.; Albertorio, F.; Kim, G.; Gurau, M. C.; Yang, R. D.; Holden, M. A.; Cremer, P. S. The Vroman Effect: A Molecular Level Description of Fibrinogen Displacement. *J. Am. Chem. Soc.* **2003**, *125*, 12782−12786.
(71) Noh, H.; Vogler, E. A. Volumetric Interpretation of Protein Adsorption: Competition From Mixtures and the Vroman Effect. *Biomaterials* **2007**, *28*, 405−422.
(72) Krishnan, A.; Siedlecki, C. A.; Vogler, E. A. Mixology of Protein Solutions and the Vroman Effect. *Langmuir* **2004**, *20*, 5071−5078.
(73) Wu, J.; Wu, Y.-Q.; Ricklin, D.; Janssen, B. J. C.; Lambris, J. D.; Gros, P. Structure of Complement Fragment C3b−Factor H and Implications for Host Protection by Complement Regulators. *Nat. Immunol.* **2009**, *10*, 728.

DOI: 10.1021/acsami.8b13749
ACS Appl. Mater. Interfaces 2018, 10, 32047−32057